Journal of Organometallic Chemistry, 448 (1993) 241–245

JOM 23229

Cyclopalladated compounds. Structural studies on dinuclear azobenzene complexes

Alessandra Crispini, Mauro Ghedini and Francesco Neve

Dipartimento di Chimica, Università della Calabria, I-87030 Arcavacata (CS) (Italy)

(Received June 29, 1992)

Abstract

The X-ray crystal structure of the cyclometallated dimer di-μ-bromo-bis[(2′,6′-dimethylazobenzenato-C^2,N^2)palladium(II)] (**2**) and its iodo analogue (**3**) are described. **2** crystallizes in the orthorhombic space group $Pca2_1$ with $a = 16.960(8)$ Å, $b = 10.251(5)$ Å, $c = 16.359(8)$ Å, $Z = 4$, $U = 2844(2)$ Å^3. Refinement of 244 parameters yielded $R = 0.074$ and $R_w = 0.081$. Crystals of **3** are orthorhombic, space group $Pca2_1$ with $a = 17.054(3)$ Å, $b = 10.506(2)$ Å, $c = 16.277(2)$ Å, $Z = 4$, $U = 2916.3(8)$ Å^3, $R = 0.033$ and $R_w = 0.036$ for 3048 reflections with $I > 3\sigma(I)$. Structural features of **2** and **3** are compared with those of the chloro homologue **1**. The possible effect of different bridging halides on the mesomorphism of related classes of compound is also discussed.

1. Introduction

Several recently synthesized dinuclear halo-bridged azo [1,2], imine [3], azine [4] or phenylpyrimidine [5] cyclopalladated complexes display thermotropic liquid crystalline properties and form a new class of material [6] suitable for electrooptical devices. The molecules of such compounds feature the $Pd_2(\mu\text{-}X)_2$ core, and, as far as mesomorphism is concerned, it has been observed that the mesomorphic behaviour somehow depends on the nature of X [3,5,7].

Since thermotropism and molecular structure are related, in order to evaluate the possible structural differences induced by the bridging halide, a single-crystal study on a homologous series of "$Pd_2(\mu\text{-}X)_2$" species is required.

The X-ray molecular structure of {[Pd(L)(μ-Cl)]$_2$} (**1**) (L is the orthopalladated form of the 2,6-dimethylazobenzene ligand), has been previously determined [8]. Although it does not exhibit mesomorphism, **1** is a representative model for investigations on the palladium-containing core. Accordingly, the related complexes {[Pd(L)(μ-X)]$_2$} (X = Br (**2**) or I (**3**)) have been considered. Here we report on their synthesis and X-ray structural analysis. Structural data on bromo- or iodo-bridged cyclopalladated azobenzenes have not yet appeared in the literature.

2. Experimental details

The complex {[Pd(L)(μ-Cl)]$_2$} (**1**) was prepared as previously described [8].

2.1. *{[Pd(L)(μ-Br)]$_2$} (2)*

A large excess (0.563 g, 5.47 mmol) of sodium bromide was added to a suspension of the chloride **1** (0.192 g, 0.27 mmol) in acetone (5 ml). After the orange solution had been stirred at room temperature for 4 h the sodium chloride was removed by filtration. The orange solid which forms upon addition of diethyl ether (20 ml) was filtered off and dried under vacuum (yield 80%). Anal. Found: C, 42.69; H, 3.28; N, 7.10. $C_{28}H_{26}Br_2N_4Pd_2$ calcd.: C, 42.50; H, 3.33; N, 7.08%. ^1H NMR ($CDCl_3$, 300 MHz): δ 7.88 (dd, 2H, $J = 7.5$, $J = 1.6$ Hz), 7.45 (br d, 2H, $J = 7.2$), 7.26–7.10 (m, 10H), 2.36 (s, 12H, CH_3).

2.2. *{[Pd(L)(μ-I)]$_2$} (3)*

A suspension of **1** (0.200 g, 0.285 mmol) in acetone (5 ml) was treated with a large excess of lithium iodide (0.762 g, 0.570 mmol). The resulting red solution was stirred at room temperature for 8 h, then the solvent evaporated under reduced pressure. The solid residue

---

Correspondence to: Professor M. Ghedini.

0022-328X/93/$6.00

was redissolved in dichloromethane and the insoluble lithium chloride was removed by filtration. The red solid which forms upon addition of ethanol (20 ml) was filtered off and dried under vacuum (yield 73%). Anal. Found: C, 37.89; H, 2.86; N, 6.22. $C_{28}H_{26}I_2N_4Pd_2$ calcd.: C, 37.99; H, 2.96; N, 6.33%. ^{1}H NMR ($CDCl_3$, 300 MHz): δ 7.94 (d, 2H, $J = 7.5$), 7.78 (br d, 2H), 7.28–7.14 (m, 10H), 2.34 (s, 12H, CH_3).

3. Crystal structure determination of 2 and 3

An orange crystal of **2** (0.50 × 0.22 × 0.40 mm) and a red crystal of **3** (0.50 × 0.85 × 0.30 mm) obtained from acetone, were used for data collection. The intensity data were collected on a Siemens R3m/V four circle diffractometer using graphite-monochromated Mo Kα radiation. Absorption corrections were applied by using the face-indexed numerical method [9] for **2** and the ψ scan method [10] for **3**. Both structures were solved by Patterson methods and completed by Fourier recycling. The Hamilton ratio test [11] was performed in order to identify the correct absolute configuration. This indicated the antipodal assignment to be correct for both crystal structures.

TABLE 1. Atomic coordinates ($\times 10^4$) and equivalent isotropic displacement coefficients ($Å^2 \times 10^3$) for complex {[Pd(L)(μ-Br)]$_2$} (**2**)

	x	y	z	U_{eq} [a]
Pd(1)	9468(1)	8590(2)	10000	58(1)
Pd(2)	8286(1)	6496(2)	11261(2)	58(1)
Br(1)	9572(2)	6296(3)	10609(3)	116(2)
Br(2)	8327(2)	8919(3)	10887(3)	91(1)
N(1)	10410(9)	8477(19)	9245(12)	55(6)
N(2)	10600(10)	9415(16)	8808(13)	52(6)
N(3)	7257(10)	6494(18)	11844(18)	71(8)
N(4)	6975(11)	5435(20)	12115(14)	61(7)
C(1)	9459(16)	10312(20)	9488(22)	82(11)
C(2)	8983(18)	11383(29)	9647(25)	93(13)
C(3)	9073(17)	12590(24)	9235(21)	77(10)
C(4)	9662(20)	12658(35)	8616(24)	107(15)
C(5)	10181(14)	11635(22)	8502(21)	70(10)
C(6)	10094(12)	10466(24)	8936(16)	58(8)
C(7)	10915(14)	7370(23)	9198(15)	57(6)
C(8)	11580(17)	7354(27)	9689(17)	71(7)
C(9)	12021(15)	6187(25)	9633(18)	67(6)
C(10)	11859(15)	5266(29)	9129(18)	73(7)
C(11)	11214(16)	5289(27)	8665(17)	71(7)
C(12)	10713(14)	6318(22)	8663(15)	54(5)
C(13)	11726(19)	8383(34)	10222(23)	96(10)
C(14)	9944(17)	6368(28)	8148(20)	82(8)
C(15)	8211(13)	4747(28)	11548(20)	77(11)
C(16)	7502(14)	4385(18)	12025(16)	56(8)
C(17)	7320(21)	3180(26)	12336(29)	108(17)
C(18)	7885(19)	2172(26)	12278(25)	95(14)
C(19)	8550(16)	2502(32)	11772(24)	93(13)
C(20)	8743(15)	3573(22)	11529(25)	87(13)
C(21)	6721(12)	7594(19)	11895(12)	44(5)
C(22)	6131(13)	7758(23)	11285(17)	62(6)
C(23)	5672(14)	8850(23)	11303(17)	63(6)
C(24)	5765(14)	9724(26)	11934(16)	66(7)
C(25)	6302(15)	9549(23)	12507(16)	64(6)
C(26)	6808(13)	8469(23)	12515(16)	56(6)
C(27)	7434(18)	8313(26)	13135(20)	78(7)
C(28)	6103(19)	6828(35)	10596(24)	95(9)

[a] Equivalent isotropic U defined as one third of the trace of the orthogonalized U_{ij} tensor.

TABLE 2. Atomic coordinates ($\times 10^4$) and equivalent isotropic displacement coefficients ($Å^2 \times 10^3$) for complex {[Pd(L)(μ-I)]$_2$} (**3**)

	x	y	z	U_{eq} [a]
Pd(1)	8292(1)	6455(1)	8683(1)	44(1)
Pd(2)	9555(1)	8610(1)	10000	44(1)
I(1)	8356(1)	8962(1)	9051(1)	62(1)
I(2)	9685(1)	6280(1)	9301(1)	90(1)
N(1)	7224(4)	6431(6)	8164(6)	47(2)
N(2)	6947(4)	5401(8)	7886(6)	53(3)
N(3)	10472(4)	8447(7)	10780(5)	47(2)
N(4)	10643(4)	9372(7)	11246(5)	50(2)
C(1)	8194(5)	4646(8)	8397(5)	45(2)
C(2)	7465(6)	4386(8)	7995(6)	51(3)
C(3)	7285(7)	3170(10)	7701(8)	72(4)
C(4)	7808(7)	2221(9)	7773(8)	71(4)
C(5)	8507(8)	2421(10)	8167(7)	71(4)
C(6)	8692(6)	3587(9)	8466(6)	52(3)
C(7)	6702(5)	7541(8)	8116(6)	46(3)
C(8)	6192(5)	7784(9)	8749(6)	56(3)
C(9)	5715(6)	8846(11)	8702(8)	70(4)
C(10)	5810(6)	9682(11)	8063(8)	73(4)
C(11)	6311(6)	9418(10)	7449(7)	68(4)
C(12)	6787(5)	8365(10)	7449(7)	54(3)
C(13)	7358(8)	8064(13)	6753(8)	85(5)
C(14)	6142(9)	6924(17)	9473(9)	108(6)
C(15)	9547(5)	10312(8)	10532(6)	44(2)
C(16)	10144(5)	10393(8)	11122(6)	50(3)
C(17)	10239(6)	11500(11)	11599(8)	68(4)
C(18)	9780(6)	12535(10)	11480(8)	66(4)
C(19)	9219(8)	12449(10)	10906(9)	83(5)
C(20)	9079(6)	11359(8)	10429(7)	55(3)
C(21)	10964(4)	7353(9)	10830(5)	46(3)
C(22)	10738(6)	6344(9)	11328(7)	56(3)
C(23)	11264(6)	5304(9)	11337(7)	60(3)
C(24)	11919(7)	5270(12)	10904(8)	76(4)
C(25)	12104(6)	6291(12)	10385(9)	72(4)
C(26)	11646(5)	7364(11)	10342(6)	56(3)
C(27)	11828(7)	8417(14)	9805(10)	93(5)
C(28)	9983(7)	6371(10)	11788(9)	75(4)

[a] Equivalent isotropic U defined as one third of the trace of the orthogonalized U_{ij} tensor.

The refinement was performed using a full-matrix least-squares procedure minimizing the function $\Sigma w(|F_o| - |F_c|)^2$. The weighting scheme was $w^{-1} = \sigma^2|F_o| + q|F_c|^2$, with q = 0.0036 for **2** and $q = 0.0002$ for **3**. While all non-hydrogen atoms of **3** were anisotropically refined, only the Pd, Br, N, and carbon atoms of the orthometallated phenyl rings were refined anisotropically for **2**. The hydrogen atoms were positioned in calculated positions with common thermal

TABLE 3. Crystal data, data collection and structure solution parameters for complexes **2** and **3**

	2	**3**
Formula	$C_{28}H_{26}Br_2N_4Pd_2$	$C_{28}H_{26}I_2N_4Pd_2$
Molecular wt	791.1	885.1
Space group	$Pca2_1$ (No. 29)	$Pca2_1$ (No. 29)
Temperature (K)	298	298
Cell dimensions:		
a, (Å)	16.960(8)	17.054(3)
b, (Å)	10.251(5)	10.506(2)
c, (Å)	16.359(8)	16.277(2)
U (Å^3)	2844.0(2)	2916.3(8)
Z	4	4
D_{calc} (g cm^{-3})	1.85	2.02
$F(000)$	1536	1680
Radiation (Å), Mo Kα	0.71069	0.71069
Scan range (deg)	$3 < 2\theta < 52$	$3 < 2\theta < 54$
Scan method	$2\theta - \theta$	$2\theta - \theta$
Independent reflns	2915	3307
Observed reflns ($3\sigma(I)$)	1860	3048
N_o/N_p	7.6	9.3
μ(Mo Kα) (cm^{-1})	40.56	33.36
Transmission factors	0.055/0.172	0.726/0.957
R [a]	0.0740	0.0334
R_w [b]	0.0807	0.0360
Goodness of fit [c]	1.47	2.37

[a] $R = \Sigma(|F_o| - |F_c|)/\Sigma|F_o|$. [b] $R_w = [\Sigma(|F_o| - |F_c|)^2/\Sigma w F_o^2]^{1/2}$.
[c] $\mathrm{GOF} = [\Sigma w(|F_o| - |F_c|)^2/(N_o - N_p)]^{1/2}$.

parameters ($U = 0.08$ Å^2). The largest and average Δ/σ during the final cycle were 0.460/0.05 for **2** and 0.131/0.027 for **3**. All calculations were performed with SHELXTL PLUS [9] and PARST [12] programs. Atomic scattering factors were as implemented in the SHELXTL PLUS program.

The final atomic coordinates and equivalent isotropic temperature factors for **2** and **3** are reported in Table 1 and Table 2, respectively. The crystallographic data for both compounds are reported in Table 3. A complete list of bond lengths and angles and of positional parameters of H atoms, structure factors and thermal parameters is available from the authors.

4. Discussion

Compounds **2** and **3** crystallize as discrete molecules, each of them being bis(μ-halo)-cyclopalladated complexes. The molecular structures and labelling schemes of {[Pd(L)(μ-Br)]$_2$} (**2**) and {[Pd(L)(μ-I)]$_2$} (**3**) are shown in Figs. 1 and 2, respectively. Selected bond lengths and angles are given in Table 4.

Crystals of **2** were not of ideal X-ray quality. Nevertheless, in spite of rather high standard deviations, the gross structural features were adequately delineated. Both **2** and **3** contain two L ligands in a geometry *trans* to the Pd–Pd vector. The atoms which form the Pd–N–N–C–C cycles are coplanar and show similar interatomic distances and angles (Table 4). The N–Pd–C bite angles are regular, with values as low as 78.2(10 °. Bond parameters within the metallacycles agree well with those usually displayed by cyclopalladated azobenzenes [8,13].

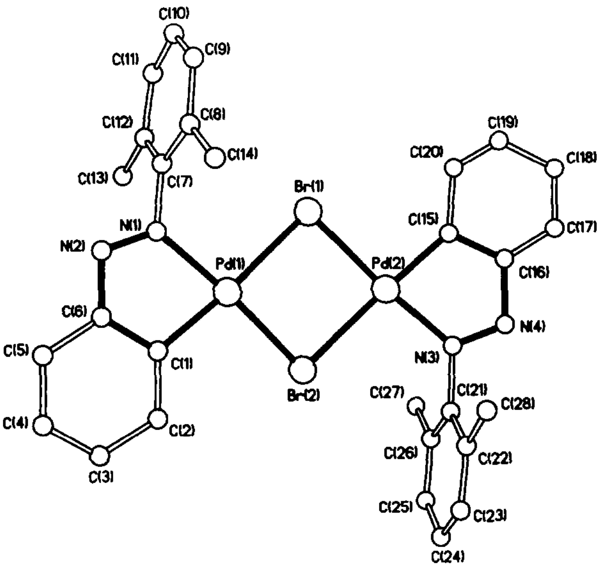

Fig. 1. Molecular structure and labelling scheme for complex **2**.

The two Pd^{II} centres in each compound have a square planar coordination. The Pd$_2$X$_2$ cores are, however, slightly folded across the X–X vector (the X---X hinged dihedral angle being 15.1(1)° for **2** and 19.8(1)° for **3**) with similar endocyclic angles (Table 4). The folding of the Pd$_2$X$_2$ unit is likely to be responsi-

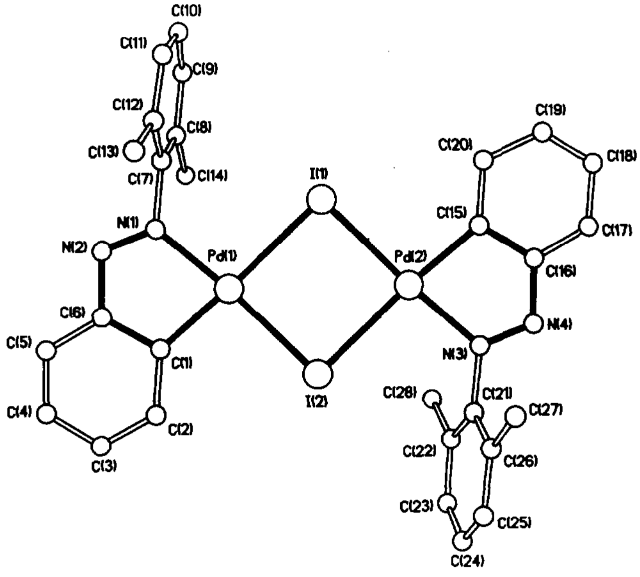

Fig. 2. A view of the structure of complex **3** showing the atomic numbering scheme.

TABLE 4. Selected bond lengths (Å) and angles (°) for complexes **2** and **3**.

	2	3
Pd(1)-X(1)	2.560(4)	2.704(1)
Pd(1)-X(2)	2.442(4)	2.587(1)
Pd(1)-N(1)	2.022(18)	2.008(7)
Pd(1)-C(1)	1.954(24)	1.964(8)
C(1)-C(6)	1.414(38)	1.430(13)
N(2)-C(6)	1.394(29)	1.396(12)
N(1)-N(2)	1.241(27)	1.265(10)
Pd(2)-X(1)	2.437(5)	2.590(1)
Pd(2)-X(2)	2.559(4)	2.708(1)
Pd(2)-N(3)	1.989(20)	2.022(7)
Pd(2)-C(15)	1.858(29)	1.987(8)
C(15)-C(16)	1.480(36)	1.402(12)
N(4)-C(16)	1.406(29)	1.385(11)
N(3)-N(4)	1.266(29)	1.266(11)
Pd(1)···Pd(2)	3.589(3)	3.790(1)
X(2)-Pd(1)-X(1)	87.2(1)	86.9(1)
X(2)-Pd(1)-C(1)	97.1(9)	95.8(3)
X(1)-Pd(1)-N(1)	97.5(6)	98.1(2)
N(1)-Pd(1)-C(1)	78.2(10)	79.1(3)
X(2)-Pd(1)-N(1)	175.3(6)	174.9(2)
X(1)-Pd(1)-C(1)	175.7(9)	177.3(3)
Pd(1)-C(1)-C(6)	111.6(17)	111.5(6)
Pd(1)-N(1)-N(2)	120.9(14)	119.9(5)
N(1)-N(2)-C(6)	110.6(19)	111.9(7)
C(1)-C(6)-N(2)	118.6(21)	117.5(7)
X(2)-Pd(2)-X(1)	87.3(1)	86.7(1)
X(1)-Pd(2)-C(15)	95.2(8)	97.3(2)
X(2)-Pd(2)-N(3)	98.0(6)	97.1(2)
N(3)-Pd(2)-C(15)	79.5(9)	78.9(3)
X(1)-Pd(2)-N(3)	174.5(6)	176.1(2)
X(2)-Pd(2)-C(15)	177.5(7)	175.6(2)
Pd(2)-C(15)-C(16)	115.5(17)	110.4(6)
Pd(2)-N(3)-N(4)	120.0(15)	119.4(6)
N(3)-N(4)-C(16)	112.3(18)	111.4(7)
C(15)-C(16)-N(4)	112.3(19)	119.9(8)

ble for non-bonding Pd–Pd separations (**2**, 3.589(3) Å; **3**, 3.790(1) Å) shorter than the corresponding distances in di(μ-bromo – bis[*N*-(3,4-dimethoxybenzylidene) cyclohexylaminato-$C^{6\prime}$,*N*]dipalladium(II) (3.631(5) Å) [14] and di(μ-iodo)bis[*o*-(di-*o*-tolylphosphino)benzyl]dipalladium(II) (3.929(1) Å) [15]. The latter are examples of cyclopalladated complexes with strictly planar Pd_2X_2 units.

The diversity in Pd–X bond length values reflects either the expected stronger *trans* influence exerted by a Pd–C(phenyl) σ bond [8,13–17] or the size of X. Single crystal X-ray analyses of cyclopalladated complexes containing the Pd_2Br_2 or Pd_2I_2 core were previously reported by Vila [13] and Rheingold [15] respectively. Those compounds are centrosymmetric. Moreover, whereas the homologous Pd–Br and Pd–I bond lengths parallel the present data, only small differences are observed in the Pd(1)–X–Pd(2) and X(1)–Pd–X(2) angles.

Since the complete series {[Pd(L)(μ-X)]$_2$} (X = Cl, Br, or I) is now to hand, a comparison of the most relevant structural features along the entire series is feasible. Whereas no significant structural differences are detected in the azo moiety L, the geometry of the Pd_2X_2 fragment changes from planar (X = Cl) to bent (X = Br or I), the folding angle being wider for X = I than for X = Br. Nevertheless, in other chloro-bridged dinuclear cyclopalladated compounds this angle is greater (*e.g.* 58° [18], 38.7(1)° [19] or 36.7(1)° [17]). Therefore the trend observed in the present case may be fortuitous and not necessarily related to the different role which each X atom plays.

In thermotropic organometallic complexes containing the Pd_2X_2 core, it has been observed that the nematic phase appears at temperatures which increase in the order Cl < Br < I [7], whereas the smetic phases show the reverse order [3,5]. Moreover, the clearing temperatures have different trends, depending on the nature of the mesogenic ligands bonded to Pd_2X_2. Thus the order is Cl < I < Br for 4-ethoxyphenylazo-4′-phenylheptanoate [7], I < Br < Cl for 5-hexyl-2-[(4′-undecyloxy)phenyl]pyrimidine [5], and Cl < Br for 4,4′-di-decyloxybenzylideneaniline [3] or 4-decyloxy-α-methylbenzylidene-4′-decylaniline [3]. Since geometrical and structural effects are not determining, a relationship between the nature of Pd_2X_2 and mesomorphic behaviour of this class of complex seems to depend on other properties of the halides (*e.g.* size, polarizability). These give rise to effects peculiar to each typical mesophase.

Acknowledgments

This work was supported by the Italian Consiglio Nazionale delle Ricerche (C.N.R.) under the "Progetto Finalizzato Materiali Speciali per Tecnologie Avanzate". We thank Johnson Matthey Research Centre, England, for a generous loan of $PdCl_2$.

References

1 M. Ghedini, S. Armentano and F. Neve, *Inorg. Chim. Acta, 134* (1987) 23 and references therein.
2 N. Hoshino, H. Hasegawa and Y. Matsumaga, *Liq. Cryst., 9* (1991) 267.
3 J. Barbera, P. Espinet, E. Lalinde, M. Marcos and J. L. Serrano, *Liq. Cryst., 2* (1987) 833.
4 P. Espinet, E. Lalinde, M. Marcos, J. Perez and J. L. Serrano, *Organometallics, 9* (1990) 555.
5 M. Ghedini, D. Pucci, G. De Munno, D. Viterbo, F. Neve and S. Armentano, *Chem. Mater., 3* (1991) 65.
6 A. M. Giroud-Godquin and P. M. Maitlis, *Angew. Chem., Int. Ed. Engl., 30* (1991) 375.
7 M. Ghedini, S. Licoccia, S. Armentano and R. Bartolino, *Mol. Cryst. Liq. Cryst., 108* (1984) 269.

8 S. Armentano, A. Crispini, G. De Munno, M. Ghedini and F. Neve, *Acta Crystallogr., Sect. C, 47* (1991) 966.

9 SHELXTL PLUS Version 4.11 (1990), Siemens Analytical X-Ray Instruments Inc., Madison, WI, USA.

10 A. C. T. North and D. C. Phillips, *Acta Crystallogr., Sect. A, 24* (1968) 351.

11 W. C. Hamilton, *Acta Crystallogr., 18* (1965) 502.

12 M. Nardelli, *Comput. Chem., 7* (1983) 95.

13 S. Armentano, A. Crispini, G. De Munno, M. Ghedini and F. Neve, *Acta Crystallogr., Sect C, 47* (1991) 2545 and references therein.

14 J. M. Vila, M. Gayoso, M. T. Pereira, A. Romar, J. J. Fernandez and M. Thornton-Pett, *J. Organomet. Chem., 401* (1991) 385.

15 A. L. Rheingold and W. C. Fultz, *Organometallics, 3* (1984) 1414.

16 N. Barr, S. F. Dike, G. Smith, C. H. L. Kennard and V. McKee, *J. Organomet. Chem., 288* (1985) 109.

17 A. Crispini, G. De Munno, M. Ghedini and F. Neve, *J. Organomet. Chem., 427* (1992) 409.

18 A. G. Constable, W. S. McDonald, L. C. Sawkins and B. L. Shaw, *J. Chem. Soc., Dalton Trans.*, (1980) 1992.

19 M. Ghedini, S. Armentano, G. De Munno, A. Crispini and F. Neve, *Liq. Cryst., 8* (1990) 739.